HHS Public Access

Author manuscript

Clin Neurophysiol. Author manuscript; available in PMC 2019 May 01.

Published in final edited form as:

Clin Neurophysiol. 2018 May ; 129(5): 909–919. doi:10.1016/j.clinph.2018.02.006.

Comparing spiking and slow wave activity from invasive electroencephalography in patients with and without seizures

Brian Nils Lundstrom, MD PhD[1], **Christian Meisel, MD PhD**[2], **Jamie Van Gompel, MD**[3], **Matt Stead, MD PhD**[1], and **Greg Worrell, MD PhD**[1]

[1]Department of Neurology, Mayo Clinic, 200 1st St SW, Rochester, MN, 55905, USA

[2]Department of Neurology, University Clinic Carl Gustav Carus, Fetscherstrasse 74, 01307 Dresden, Germany

[3]Department of Neurosurgery, Mayo Clinic, 200 1st St SW, Rochester, MN, 55905, USA

Abstract

Objectives—To develop quantitative measures for estimating seizure probability, we examine intracranial EEG data from patient groups with three qualitative seizure probabilities: patients with drug resistant focal epilepsy (high), these patients during cortical stimulation (intermediate), and patients who have no history of seizures (low).

Methods—Patients with focal epilepsy were implanted with subdural electrodes during presurgical evaluation. Patients without seizures were implanted during treatment with motor cortex stimulation for atypical facial pain.

Results—The rate and amplitude of spikes correlate with qualitative seizure probability across patient groups and with proximity to the seizure onset zone in focal epilepsy patients. Spikes occur earlier during the negative oscillation of underlying slow activity (0.5–2 Hz) when seizure probability is increased. Similarly, coupling between slow and fast activity is increased.

Conclusions—There is likely a continuum of sharply contoured activity between non-epileptiform and epileptiform. Characteristics of spiking and how spikes relate to slow activity can be combined to predict seizure onset zones.

Significance—Intracranial EEG data from patients without seizures represent a unique comparison group and highlight changes seen in spiking and slow wave activity with increased seizure probability. Slow wave activity and related physiology are an important potential biomarker for estimating seizure probability.

Corresponding Authors: Brian Lundstrom, Department of Neurology, Mayo Clinic, 200 1st St SW, Rochester, MN, 55905, Phone: 507-284-8687, Fax: 507-284-8686, lundstrom.brian@mayo.edu.

Conflict of Interest Statement

Dr. Lundstrom and Dr. Meisel have no potential conflicts of interest to be disclosured. Dr. Van Gompel, Dr. Stead, and Dr. Worrell hold stock options with Cadence Neuroscience, Inc.

Keywords

EEG; Epilepsy monitoring

Introduction

Seizures have long been defined as paroxysmal events typified by abnormally excessive or synchronous brain activity (Fisher et al., 2005). Seizures can occur in healthy brain, or can be the result of disease. By definition, epilepsy requires an increased probability of seizures. Seizure threshold is a clinically useful concept expressing a time-varying probability of seizures. Despite clinical relevance, there remains no clear way of quantitatively assessing seizure probability. As a result, epilepsy patients often undergo long therapy titrations or never have their therapy appropriately optimized. There is a need for improved estimates of seizure probability to guide pharmacological and stimulation therapy as well as an improved understanding of the differences of brain physiology between patients with and without seizures.

To examine potential biomarkers for seizure probability, we consider data from intracranial electroencephalography (iEEG), which generally provides higher fidelity signals than scalp EEG (Nunez and Srinivasan, 2006). We would like to examine data from patients who have a high, intermediate, and low probability of having seizures. For the high seizure probability group, we use iEEG data from focal drug resistant epilepsy patients upon initial admission to the epilepsy monitoring unit. For these patients, grids were implanted over the primary motor cortex ($n = 5$), posterior temporal lobe ($n = 1$), and parietal lobe ($n = 1$).

For the intermediate seizure probability group, we use data from these same patients later during their hospital stay when they were treated with Chronic Subthreshold Cortical Stimulation (CSCS) (Lundstrom et al., 2016). In general, drug-resistant focal epilepsy patients undergo evaluation with iEEG to assess whether they are candidates for resective surgery, typically the most effective therapy (Wyllie, 2015). If they are not, brain stimulation techniques offer an alternative (Gschwind and Seeck, 2016; Lundstrom et al., 2017). CSCS is a novel brain stimulation technique that provides continuous electrical stimulation to a focal area of cortex (Child et al., 2014; Kerezoudis et al., 2017; Lundstrom et al., 2017, 2016). Prior work shows that cortical stimulation lowers seizure probability (Elisevich et al., 2006; Lundstrom et al., 2016; Velasco et al., 2000).

For the low seizure probability group, we want iEEG data from patients who have no history of seizures. Invasive monitoring is not typically performed for patients without a seizure history given the associated morbidity. However, patients with refractory facial pain are occasionally implanted for motor cortex stimulation (Thomas et al., 2009). Here, we use iEEG obtained from subdural grids implanted over the motor cortex during their clinical evaluation prior to electrical stimulation and permanent implantation. Thus, we can examine iEEG measures from patients with a high, intermediate, and low seizure probability.

Our goal is to examine the characteristics of spiking activity and underlying slow oscillations as seizure probability varies to find potential biomarkers to estimate seizure

threshold. Recent work has suggested that EEG-related measures such as spatial synchrony of oscillation phase can increase over time with reductions of anti-seizure medications or prolonged wakefulness (Meisel et al., 2015). Although spike rates can increase or decrease in pre-ictal time periods (Karoly et al., 2016), our motivation for examining spiking activity extends to prior observations that spiking rates correlate with seizure activity in the setting of cortical stimulation (Elisevich et al., 2006; Velasco et al., 2000), and our ongoing clinical practice of using spiking activity to guide parameter adjustments during cortical stimulation (Lundstrom et al., 2017, 2016). Our motivation for examining slow oscillations stems from evidence that the phase of slow wave activity modulates cortical excitability and the timing of epileptiform discharges (Frauscher et al., 2015; Vanhatalo et al., 2004). Since the focal epilepsy patients have clinically defined SOZs, we can correlate changes between patient groups with changes noted within and outside the SOZ. We hypothesized that measures of seizure probability will vary between the three patient groups (low, intermediate and high seizure probability), and that in epilepsy patients the measures will correlate with proximity of electrodes to the SOZ.

Methods

Patients

Intracranial electroencephalography (iEEG) data were analyzed with Mayo Clinic IRB approval from thirteen distinct patients. Data from patients with drug-resistant focal epilepsy ($n = 7$, 4 females) were divided into two groups: data were recorded upon admission (EpiAdm, $n = 7$) and following the initiation of cortical stimulation (EpiStim, $n = 7$). During cortical stimulation anti-seizure medications were either the same as EpiAdm or reduced by approximately 30–50%. Data from patients with intractable facial pain (FcPain, $n = 6$, 4 females) did not have any history of seizures. These patients were prophylactically treated with an anti-seizure medication, typically phenytoin, initiated during their hospital stay given an increased risk for stimulation-induced seizures (Thomas et al., 2009). Epilepsy patients were evaluated for potential surgical resection with surgically implanted subdural grid electrodes over the fronto-parietal ($n = 5$), temporal ($n = 1$), or parieto-occipital ($n = 1$) regions. All patients were unsuitable resection candidates since the seizure onset zone (SOZ) was in eloquent motor ($n = 5$, face or upper limb), language ($n = 1$), or visual ($n = 1$) cortex. They received a therapeutic trial of continuous subthreshold cortical stimulation (biphasic, 2 Hz, pulse width 90–450 μs, amplitude 1–6 V in voltage mode) via subdural grid electrodes in the SOZ (Lundstrom et al. 2016). Patients with refractory facial pain were implanted with subdural grid electrodes over the fronto-parietal region including the motor cortex for a trial of therapeutic stimulation (Thomas et al. 2009).

Experimental design and statistical analysis

Data were acquired with either a Natus EMU 128Fs (bandwidth 0.1 to 940 Hz) or Neuralynx ATLAS Hybrid (bandwidth 0.16 to >1000 Hz) electrophysiology system. For each data group EpiAdm (high seizure probability), EpiStim (intermediate seizure probability), and FcPain (low seizure probability), 500 Hz iEEG data from 4×4 subdural grids of clinical macroelectrodes (4.2 mm^2, 10 mm spacing) were analyzed. Although some epilepsy patients were implanted with larger grids, a 4×4 grid including the SOZ was chosen to maintain

sampling uniformity. Six fifteen-minute blocks of data were obtained at approximately two-hour intervals between 8 pm and 6 am for 144–168 hours of iEEG data. For EpiAdm and FcPain, data were collected over the first night in the hospital. Individual channels with pervasive artifacts were removed, amounting to approximately 2% of the collected data. Sharply contoured waveforms were detected as spikes via a previously validated method (Barkmeier et al., 2012). Briefly, for each 1-minute block of data, candidate spikes are detected via a threshold defined by standard deviations (SD coefficient) of the absolute amplitude of high bandpass filtered EEG signal (20–50 Hz) for the channel. Shape criteria of amplitude, duration, and slope is applied to a lower bandpass filtered EEG signal (1–35 Hz) that is normalized to the grid as follows: for each channel, the time average of the absolute amplitudes is found, and the normalization factor is the median value of these average absolute amplitudes across all channels in the grid. Spike duration was determined by searching 40 ms on either side of the detected peak to find the minima on each side. This trough search parameter was increased only for illustrative purposes in Figure 1. Spike times are then generated with associated shape characteristics of amplitude, width and slope. Standard parameters with the previously used scaling factor 70 were used (Barkmeier et al., 2012): SD coefficient = 4, slope = 7/70 = 0.1, and duration = 20 ms. The prior study used an amplitude threshold of 600/70 = 8.6, which is the sum of the left and right amplitudes of the candidate spike. Here, we used a higher threshold of 1400/70 = 20, which equals an average spike height of 10. Amplitudes are normalized to units of the median (for the grid) of the average (over time) absolute amplitudes for each channel. The higher threshold parameter was used with the realization that this spike detection algorithm detects about 40% more spikes than reviewers (Barkmeier et al., 2012) and with the desire to be more selective.

Given the cortical stimulation and related artifact during the EpiStim group, two steps were taken to minimize artifact. First, due to the 2-Hz stimulation frequency, spike time differences of 2, 1, and 0.5 Hz were removed with a jitter of 2 ms allowed. Second, for each one-minute block of data, during spike detection a minimum threshold is defined as four standard deviations of the absolute amplitude for a given channel, as described above. However, if this threshold was too high, then that 1-minute of data for the channel was excluded. Specifically, if the threshold was greater than 7 grid normalized units (defined as above), the data were excluded. Typical threshold values were ~2–2.5, so this had the effect of excluding data with a defined threshold ~3 times greater than average, i.e. data blocks with unusually large voltage excursions related to artifact. These two steps were applied to all data and did not appreciably affect either the EpiAdm or FcPain groups. 95% confidence intervals (bias corrected and accelerated) were obtained by bootstrapping with 10,000 iterations, which provides a nonparametric and robust confidence interval estimate (Press, 1992).

Seizure onset zones

For EpiAdm, the seizure onset zone (SOZ) was determined from clinical reports describing the contacts involved within the initial second of seizure onset. Of the 16-contact grid considered for each patient, the SOZ included 4, 3, 3, 4, 2, 2, and 6 contacts for the seven patients, respectively. Bridge channels were defined as channels adjacent to the SOZ, and

nSOZ channels were the remaining contacts of the 16-contact grid. The nSOZ channels included 4, 6, 9, 5, 9, 8, and 4 contacts for each of the seven patients, respectively.

Slow wave phases and synchrony measures

To reduce artifact and intergroup differences related to reference placement, the average of all iEEG channels was subtracted from each channel prior to further analysis. This is identical to an average referential montage, as often used clinically. For all frequency bands, iEEG data were filtered forward and backwards to preserve phase using fourth-order butterworth filters. The Hilbert transform was used to obtain the discrete-time analytic signal, and the phase angle of this signal represents the instantaneous phase of the dominant frequency within the passband of the signal.

To calculate the cross-frequency coupling using the Synchronization Index (SI) (Cohen, 2008), phases were obtained for slow oscillations θ_L (0.5–2 Hz) and for the envelope of higher frequency activity θ_H. To find θ_L, data were bandpass filtered between 0.5–2 Hz with a zero-phase filter and the instantaneous phase found, as above. To find θ_H, bandpass data were Hilbert transformed and the phase taken of the resulting time-varying power series. The SI is then defined to be $|\sum e^{i(\theta_L - \theta_H)}|/N$, where N is number of time points and θ is the instantaneous phase. SI is calculated for each contact, and is equivalent to one minus the circular variance of the phase difference $\theta_L - \theta_H$ (Zar, 2009), and is a measure of the concentration of the phase differences. As SI increases, the dispersion and circular standard deviation of the phase difference decreases. Mean Phase Coherence (MPC) (Mormann et al., 2000) has a similar form to SI. Instead of considering phase differences between frequency bands, phase differences are taken between the phases θ_1 and θ_2 of two adjacent electrodes. Thus, for a given frequency band, MPC is defined to be $|\sum e^{i(\theta_1 - \theta_2)}|/N$, where N is the number of time points. MPC is calculated for each of the 24 adjacent pairs in the 16 contact-grid for each of the six fifteen-minute blocks for each patient.

Predicting contacts involved in the SOZ

Each of the 16 contacts in a subdural grid was assessed for four measures: increased spike rate, increased spike amplitude, early spike phase relative to the underlying surface negative slow oscillation (0.5–2 Hz), and increased Synchronization Index (12–20 Hz). These measures were calculated for each contact in the grid. Then, for each measure, the contacts were ranked from 1 to 16. This ranking was summed across measures generating a score with minimum and maximum values of 4 and 64, respectively. The two contacts with the lowest score for each grid were labelled the predicted SOZ, which was compared to the clinically determined SOZ. A Monte Carlo simulation (n = 10,000) was used to determine the chance probability that the predicted SOZ matched the clinically determined SOZ.

Results

Characteristics of spiking and slow activity from intracranial electroencephalography (iEEG) were analyzed for three data groups: focal drug-resistance epilepsy patients upon admission (EpiAdm, n = 7), these same epilepsy patients after the initiation of cortical stimulation

(EpiStim, $n = 7$), and patients with intractable pain and no history of seizures (FcPain, $n = 6$).

Sharply contoured waveforms detected as spikes

Sharply contoured waveforms were detected by a previously validated method for identifying iEEG spikes (Barkmeier et al., 2012). After meeting threshold criteria (see Methods), candidate spikes then met shape criteria for amplitude (>10), slope (>0.1), duration (20–80 ms) (Fig. 1a, within dashed area). Units for amplitude and slope are normalized to the grid median of the time average of the absolute amplitude of each contact. Similar to typical definitions of spikes, the duration is restricted to 20–80 ms, i.e. 12.5–50 Hz. Between the three patient groups, differences in shape characteristics are readily apparent for duration and amplitude (Fig. 1b). The bimodal shape of the duration distribution of EpiAdm candidate spikes in Fig. 1b is related to a population of somewhat broader spikes as well as spikes associated with underlying slow waves. If these candidate spikes met amplitude and slope criteria without the underlying slow waves, they were still counted as spikes when the duration criteria was narrowed (see Methods). Although waveforms may meet these objective criteria and be labeled as spikes, we are not suggesting that they are all seizure-related or epileptiform. Rather, we are seeking an unbiased and objective means of classifying brief sharply contoured waveforms, so that we may examine differences between patient groups.

Spike rate is higher in the EpiAdm than EpiStim or FcPain groups

For each patient, sharply contoured waveforms were detected and labeled as spikes (Fig. 2a and Fig. 2b). Spike rates varied from more than 10 spikes per minute in some channels from EpiAdm to a typical rate of about 0.1 spikes per minutes in FcPain (Fig. 2c). That there continued to be sharply contoured waveforms identified as spikes in patients without a seizure history highlights an ambiguity inherent in identifying spikes by objective criteria. This also suggests that the sharply contoured waveforms identified as spikes occurring in the FcPain group are unlikely to be epileptiform, given that these patients are without a seizure history. The mean spike rates calculated for each contact were then considered across patient groups. Overall mean spike rates were significantly higher in EpiAdm compared to EpiStim and FcPain (Fig. 2d), consistent with prior results (Lundstrom et al., 2016). Spike rates within each group were similar for the six recorded time epochs. Given long-tailed distributions, median values of spike amplitudes were considered for each patient group. Amplitudes were significantly different, although the median spike amplitude differences were small (Fig. 2e).

Spike rate is higher in the SOZ compared to the nSOZ

Contacts within the seizure onset zone (SOZ) were identified from clinical EEG reports. Bridge channels were defined as the direct neighbors to the SOZ, while non-SOZ (nSOZ) channels were at least one contact removed from the SOZ (Fig. 3a). Mean spike rates were calculated for SOZ channels, Bridge channels, and nSOZ channels for each time block. The spike rates were significantly increased for SOZ channels compared to nSOZ channels (Fig. 3b). At the patient level, mean spike rates were calculated for SOZ and Bridge contacts, or peri-SOZ region, and normalized by the mean rate of the nSOZ contacts for each patient. A

normalized rate greater than one signifies an increased number of spikes in the SOZ and Bridge regions. Rates were significantly increased in the peri-SOZ compared to the nSOZ for five of seven patients (Fig. 3c). The two patients without significantly increased rates had SOZs in the left perirolandic region involving eloquent motor cortex and imaging consistent with a focal cortical dysplasia (n =1) and trauma-related encephalomacia (n = 1).

Median spike amplitudes in the SOZ were increased compared to those from Bridge contacts, which were in turn increased compared to nSOZ. (Fig. 3d). Although significant, amplitude differences were small. However, the distribution of SOZ amplitudes has a long rightward tail showing an increased number of high amplitude spike outliers (Fig. 3e). Thus, the rare presence of very large amplitude spikes could help differentiate the SOZ. Prior work has suggested that higher amplitudes can help distinguish pathological high frequency oscillations (HFOs) from physiologically-induced oscillations (Kucewicz et al., 2014; Matsumoto et al., 2013).

Overall, these results are consistent with spikes that are more frequent within the SOZ compared to the nSOZ, and with the presence of rare high amplitude spikes in the SOZ. These data do not support the notion that spike rate is necessarily increased in the SOZ for every patient, as this was not the case for two of the seven patients. However, in none of the cases were spike rates significantly increased in the nSOZ (Fig. 3c), and spikes rates were often 10 to 100-fold higher in the peri-SOZ. Thus, the presence of contacts with significantly increased rates may be more helpful then their absence.

Spikes occur earlier in the negative portion of slow oscillations for SOZ and EpiAdm

Prior work suggests that the negative phase of underlying slow oscillations is related to cortical excitability (Vanhatalo et al., 2004) and that HFOs occurring in the SOZ occur earlier in the negative phase than those outside the SOZ (Frauscher et al., 2015). Here, we wanted to relate spike times to slow oscillations (0.1–2 Hz) (Fig. 4a), where the negative peak for the slow oscillations is taken to have a phase of zero degrees. The peak probability for spikes from the SOZ was approximately 60 degrees earlier than for spikes in the nSOZ (Fig. 4b). In other words, the peak firing probability for SOZ spikes occurred earlier during the negative phase of the slow oscillation potentials than for nSOZ spikes (Fig. 4b, left panel). A second peak for SOZ spikes at approximately 130 degrees occurred prior to the maximal positive potential of the slow oscillation. When considering phases during the negative oscillation, i.e. −90 to 90 degrees, median phases occurred significantly earlier for the SOZ than for Bridge or nSOZ. A similar trend was present when comparing spike phases from EpiAdm to EpiStim and FcPain (Fig. 4c). Spike phases within each group did not change significantly over the course of the night. Thus, spikes associated with patients or cortical regions with higher seizure probability occurred earlier during the negative portion of slow oscillations (0.5–2 Hz).

Cross-frequency coupling is increased in the SOZ and for epilepsy patients

Given prior work suggesting that slow oscillations may modulate higher frequency activity (Frauscher et al., 2015; Vanhatalo et al., 2004) as well as the above results relating spike timing to the slow oscillation phase, we wanted to look further at how slow oscillations are

related to higher frequency bands. Multiple methods exist for examining cross-frequency coupling, such as phase amplitude coupling (Canolty et al., 2006). Here, we used a Synchronization Index (Cohen, 2008), which has a straightforward interpretation and effectively measures the circular variance of phase differences between two frequency bands. The SI is higher when the circular variance is lower, as is the case when the phase differences are more concentrated rather than uniformly distributed. We examined the SI between slow oscillations (0.5–2 Hz) and five higher frequency bands: 4–8, 8–12, 12–20, 20–50, and 70–110 Hz. Within the EpiAdm group, the SI was significantly increased for the SOZ compared to the nSOZ for all frequencies (Fig. 5b). The preferred slow oscillation phase at which coupling was maximal was significantly earlier during the negative oscillation for the frequency band 70–110 Hz (Fig. 5b, right panel). Similar results were present when comparing EpiAdm to FcPain. SI was significantly increased for all frequency bands for EpiAdm compared to FcPain. The preferred phase for coupling was not significantly different between the two groups. EpiStim data were not considered insofar as ongoing stimulation induces artifact that artificially increases coupling and synchrony.

These results suggest a relationship between the slow oscillation band and higher frequency bands. Specifically, for cortex that has a higher probability of generating seizures there is a tighter coupling between low and high frequencies. Here, the cortex in these results is restricted to neocortex. For higher frequency bands, a greater portion of the preferred phases occur during the positive oscillation (data not shown), consistent with prior data suggesting that the negative oscillation corresponds to a “down” state, or period of reduced activity, for high frequency activity (Frauscher et al., 2015; Steriade, 2006).

Mean phase coherence is increased for patients without seizures

Cross-frequency coupling can be thought of as assessing synchrony between frequency bands of a given contact, and does not assess spatial synchrony. Recently, synchrony was assessed across channels over time for single patients with a synchrony measure R (Meisel et al., 2015), which is related to the circular variance of all phases across channels at a given time point. Synchrony increased over time with the withdrawal of anti-seizure medications and sleep deprivation. Because R is very sensitive to inter-electrode distance as well as the number of electrodes, here we used mean phase coherence (Mormann et al., 2000), a related measure that is essentially the circular variance of the phase difference between pairwise contacts.

We found the MPC of the 24 adjacent contact pairs for six frequency bands: 0.5–2, 4–8, 8–12, 12–20, 20–50, and 70–110 Hz. MPC was calculated for 15-minute blocks and then averaged for the six blocks spanning the approximately 10-hour period. Although the average MPC was significantly increased for nSOZ contacts at frequencies >20 Hz (Fig. 6a), significant variability exists at the patient level with no definite trend in either direction evident (Fig. 6b). For each patient, the average of the MPC for SOZ and Bridge contacts was divided by the average of the MPC for the nSOZ and is shown for the frequency bands 20–50 and 70–110 Hz.

The average MPC was decreased for EpiAdm compared to FcPain for all frequencies (Fig. 6c) with example distributions shown for the lowest and highest frequency bands (Fig. 6d).

Similar results were obtained when using the median MPC instead of the average, when excluding the two EpiAdm patients with SOZ outside of primary motor cortex, and when using zero-lag pairwise cross-correlations (data not shown). One interpretation of this data is that decreased spatial synchrony is more closely tied to exposure to anti-seizure medications, rather than seizure probability. This would be consistent with earlier observations that anti-seizure medications reduce synchrony in cortex (Meisel et al., 2015), and here EpiAdm patients were exposed to a high load of anti-seizure medications relative to FcPain patients.

Predicting contacts involved in the SOZ

To demonstrate the potential for these measures to be predictive of contacts located in the SOZ, we ranked the 16 electrodes in each EpiAdm grid from most likely to be in the SOZ to least likely (Figure 7). Each contact was assessed using four of the measures described above: highest spike rate, highest spike amplitude, earliest spike phase relative to the slow negative oscillation (0.5–2 Hz), and highest Synchronization Index (12–20 Hz). These were chosen according the above results and equally weighted. The predicted channels matched the clinically determined SOZ channels in eight of the 14 possible channels, which occurred by chance in approximately 0.003 of trials during a Monte Carlo simulation (n = 10,000).

Discussion

The objective of this study is to examine the characteristics of spiking and related slow oscillations in invasive EEG (iEEG) data from patients with a high, intermediate, and low seizure probability. We find that in the group with highest seizure probability (EpiAdm) and near the SOZ: 1) spike rates and amplitudes were increased, 2) spikes occurred earlier during the negative portion of slow oscillations, and 3) coupling between slow oscillations and higher frequency activity was increased. Results support the hypotheses that these measures correlate with seizure probability between patient groups and spatially with respect to the SOZ, and that multiple measures used in conjunction may be more effective for predicting seizure probability.

To our knowledge this is the first investigation of seizure probability using a systematic analysis of iEEG data including a comparison group without a seizure history. By comparing results with this low seizure probability group, it becomes clearer that spike rate and amplitude, rather than simply the presence of sharply contoured activity, may have more relevance for quantifying seizure probability. Similarly, the importance of slow wave physiology may be underappreciated.

Although facial pain patients have a very low *a priori* seizure probability, as they have no history of seizures, their motor cortex physiology may be abnormal. The mechanism by which motor cortex stimulation alleviates atypical pain is unclear (Thomas et al., 2009). One theory is that applied stimulation to the presumed normal primary motor cortex effectively inhibits abnormal excitation in the primary somatosensory cortex. Another consideration is that the placement of subdural grids may lead to cortical injury that alters excitability. Clinically, it has long been noted that cortical manipulation and acute trauma can reduce seizure probability (Jerome Engel, 2013), sometimes termed a “lesional” effect after placement of leads for deep brain stimulation (Li and Cook, 2017). This type of alteration

might be expected to occur somewhat uniformly over all involved areas. Regardless, any effect from cortical manipulation and grid placement should be similar for EpiAdm and FcPain, and might be expected to affect contacts in the SOZ and nSOZ similarly.

All patients were on anti-seizure medications. Overall medication dosages were highest in the EpiAdm group, as they were typically on multiple medications which were typically reduced modestly for their first hospital night. Medications dosages were similar for EpiStim, or somewhat lower. As a part of clinical practice, we typically keep anti-seizure medications reduced during initial stimulation to assist with stimulation parameter optimization (Lundstrom et al., 2017, 2016). For FcPain, patients were prophylactically started on one anti-seizure medication the night of their admission, to reduce the risk of a stimulation-induced seizure (Thomas et al., 2009). Given that anti-seizure medications tend to lower seizure probability, the above differences in anti-seizure medication loads would if anything act counter to the observed results, lessening differences between patient groups.

These data are limited by a small number of patients in which invasive sampling is determined by clinical indication. Five of the seven epilepsy patients had grids over primary motor cortex, while one had a grid over the posterior temporal lobe and another over the parieto-occipital region. The pain patients all had implants over the primary motor cortex, although the precise location of the grids varied in terms of frontal and parietal coverage. The small number of patients here unfortunately does not allow for meaningful subgroup analyses such as stratification of our results by lobe or pathology.

Sharply contoured activity detected as spikes

Whether interictal EEG findings can be used to predict epilepsy has been questioned for years, although more recent evidence demonstrates that the presence of spikes (Staley et al., 2011) and changes in spike morphology (Huneau et al., 2013) precede epilepsy in rodent models. Prior work in human recordings suggests iEEG spikes from patients without epilepsy have a reduced after-coming slow wave and are more localized (Janca et al., 2015). Other work suggests some degree of epileptiform-like activity, such as microseizures, exist in patients without a seizure history (Stead et al., 2010). Regarding scalp EEG, a rate of greater than 60 temporal lobe spikes per hour predicted a worse surgical outcome following temporal lobectomy (Krendl et al., 2008). Regarding invasive data, during CSCS decreased rates of iEEG spikes appear to correlate with stimulation efficacy and reduced seizures (Elisevich et al., 2006; Lundstrom et al., 2016; Velasco et al., 2000).

Here, results suggest that the rate of sharply contoured waveforms in iEEG data correlate with seizure probability, at least in some patients. That sharply contoured activity was detected as spikes in patients without a seizure history suggests that relating these detected spikes directly to epileptiform activity would be presumptuous. Rather, these spikes are better considered to be of unclear significance, somewhat similar to other well-known EEG variants of sharply contoured activity such as phantom spike and wave discharges. In general, one of the limitations to using sharply contoured waveforms, or spikes, as a biomarker is that the underlying physiology of what constitutes an epileptiform versus non-epileptiform waveform is unclear. Our intent here is to employ a straightforward definition

of sharply contoured activity, and examine the related characteristic of this “spiking” activity. We do not intend to imply that the whole of this activity is epileptiform.

It is well known that the clinical determination of what is epileptiform can be highly subjective. While some detected waveforms may not be deemed epileptiform by human observers, one benefit of automated detection is consistency. Benefits of the above spike detector (Barkmeier et al., 2012) include straightforward criteria to detect spikes and thresholding criteria that account for the amplitude of all channels rather than a single channel. However, one potential limitation is that it does not account for the presence or shape of any after-coming slow waves. Thus, we re-analyzed spike counts for EpiAdm and FcPain using a spike detector that accounts for related slow waves and the related disruption of the background (Janca et al., 2015). The trend was the same as Figure 2d with the previous detector; for example, with parameter k1=5, EpiAdm (n = 112; 2.3, [1.2 4.0]) and FcPain (n = 96; 0.39, [0.25 0.83]). In short, as suggested by Figure 1a, there may not be a straightforward way to delineate epileptiform and non-epileptiform spikes. Intracranial spikes may exist on a continuum of epileptiform and non-epileptiform.

Spikes related to slow oscillation phase

Prior work suggests that underlying slow waves (0.01–0.2 Hz) modulate faster activity, such as sleep architecture and interictal spikes (Vanhatalo et al., 2004), and can assist in localizing the SOZ (Miller et al., 2007). Similarly, spikes and HFOs were seen during the surface negative phase of slow oscillations (0.3–4 Hz), where HFOs occurred earlier in the negative phase for SOZ compared to nSOZ channels (Frauscher et al., 2015). In this study, spikes from EpiAdm in general and specifically the SOZ occurred early in the surface negative phase of the slow oscillations (0.5–2 Hz). This suggests that an early negative phase may not only relate specifically to the SOZ but could serve as a more global marker related to increased excitability.

The surface negative portion of slow oscillations is thought to be related to periods of relative inactivity, or down states, in higher frequency bands (Contreras and Steriade, 1995; Frauscher et al., 2015; Steriade, 2006), with decreased single unit activity noticed during slow waves of sleep (Nir et al., 2011). Phase changes of activity occurring during down states may suggest changes in the mechanisms of neural excitability that control up to down state transitions (Neske, 2015). The bimodal distribution seen in Fig 4c and 4d suggests there are two clusters of spikes, those that occur just prior to the surface negative oscillation and those that occur just prior to the surface positive oscillation. The significance of the two clusters is unclear. Related work has suggested a similar bimodal distribution for HFOs (Song et al., 2017). However, in that work the HFO cluster during the down-up transition was concluded to be less likely pathologic. Thus, an analogous interpretation for these spike clusters is less likely. Here, the spike cluster during the surface positive oscillations seems to be related to the overall increased probability for spiking observed in SOZ contacts.

Cross-frequency coupling and mean phase coherence

A more systematic means of assessing relationships between slow oscillations and higher frequency activity such as spikes is via measures of cross-frequency coupling. Here, we use

the Synchronization Index (Cohen, 2008), which has the advantage of a straightforward interpretation and essentially measures the circular variance of phase differences between two frequency bands. While cross-frequency coupling essentially assesses temporal synchrony between low and high frequency bands, mean phase coherence (MPC) (Mormann et al., 2000) assesses spatial synchrony between two electrodes. Together SI and MPC can be thought of as measures that assess the temporal and spatial relationships in the iEEG data, respectively. Our results suggest that increased seizure probability may affect coupling strength in a frequency-independent manner and coupling phase in a frequency-dependent manner (Fig. 5b, right panel), which potentially relate to underlying changes in neuronal excitability.

When we examined spatial synchrony with MPC between adjacent contact pairs, we found overall increased synchrony for FcPain patients compared to EpiADM. At the patient level MPC values were significantly increased or decreased in the nSOZ, depending on the patient. Prior work using a related synchrony measure R found increased global spatial synchrony as anti-seizure medications were withdrawn and with sleep deprivation (Meisel et al., 2015). Other work has shown both reduced synchrony at the SOZ (Warren et al., 2010) as well as increased spatial synchrony (Klimes et al., 2016).

Taken together, these results are in line with the notion that high loads of anti-seizure medications lead to decreased spatial synchrony in cortex (Meisel et al., 2015). They further highlight the potential sensitivity of these types of measures to details of methodology and individual patient characteristics. Some synchrony measures may be better suited for intra-patient comparisons.

Using measures to predict increased seizure probability

In the evaluation of focal drug resistant epilepsy patients for possible surgical resection, one of the primary challenges is to precisely localize the epileptogenic zone. Thus, there are clear benefits to predicting areas of increased seizure probability. Here, we used the SOZ as a proxy for the epileptogenic zone and found that a combination of measures has the potential to predict the SOZ in a proof of concept analysis. A clear limitation here is uncertainty regarding the location of the defined SOZ relative to the epileptogenic zone, as data regarding clinical outcomes are not available. The advantages of estimating seizure probability are not limited to spatial localization. A principle challenge in medical therapy titration or the adjustment of brain stimulation parameters is estimating seizure threshold, or seizure probability. Estimating seizure frequency is difficult, inefficient, and often presupposes that a well-defined seizure type represents the extent of disease burden. Improved ways to estimate seizure threshold are needed to increase treatment efficacy. The characteristics of spiking and their relationships to underlying slow activity are potential biomarkers for estimating seizure threshold.

Acknowledgments

Data collection was supported by grant NIH UH2-NS095495 (GW) as well as the generous assistance of Drs. Kendall Lee and Nicolas Wetjen (Department of Neurosurgery, Mayo Clinic, Rochester, MN) and Cindy Nelson (Department of Neurology).

Funding

Data collection was supported by grant NIH UH2-NS095495 (GW).

References

Barkmeier DT, Shah AK, Flanagan D, Atkinson MD, Agarwal R, Fuerst DR, et al. High inter-reviewer variability of spike detection on intracranial EEG addressed by an automated multi-channel algorithm. Clin Neurophysiol. 2012; 123:1088–95. DOI: 10.1016/j.clinph.2011.09.023 [PubMed: 22033028]

Canolty RT, Edwards E, Dalal SS, Soltani M, Nagarajan SS, Kirsch HE, et al. High Gamma Power Is Phase-Locked to Theta Oscillations in Human Neocortex. Science. 2006; 313:1626–8. DOI: 10.1126/science.1128115 [PubMed: 16973878]

Child ND, Stead M, Wirrell EC, Nickels KC, Wetjen NM, Lee KH, et al. Chronic subthreshold subdural cortical stimulation for the treatment of focal epilepsy originating from eloquent cortex. Epilepsia. 2014; 55:e18–21. DOI: 10.1111/epi.12525

Cohen MX. Assessing transient cross-frequency coupling in EEG data. J Neurosci Methods. 2008; 168:494–9. DOI: 10.1016/j.jneumeth.2007.10.012 [PubMed: 18061683]

Contreras D, Steriade M. Cellular basis of EEG slow rhythms: a study of dynamic corticothalamic relationships. J Neurosci. 1995; 15:604–22. [PubMed: 7823167]

Elisevich K, Jenrow K, Schuh L, Smith B. Long-term electrical stimulation-induced inhibition of partial epilepsy. Case report J Neurosurg. 2006; 105:894–7. DOI: 10.3171/jns.2006.105.6.894 [PubMed: 17405261]

Fisher RS, van Boas WE, Blume W, Elger C, Genton P, Lee P, et al. Epileptic Seizures and Epilepsy: Definitions Proposed by the International League Against Epilepsy (ILAE) and the International Bureau for Epilepsy (IBE). Epilepsia. 2005; 46:470–2. DOI: 10.1111/j.0013-9580.2005.66104.x [PubMed: 15816939]

Frauscher B, von Ellenrieder N, Ferrari-Marinho T, Avoli M, Dubeau F, Gotman J. Facilitation of epileptic activity during sleep is mediated by high amplitude slow waves. Brain. 2015; 138:1629–41. DOI: 10.1093/brain/awv073 [PubMed: 25792528]

Gschwind M, Seeck M. Transcranial direct-current stimulation as treatment in epilepsy. Expert Rev Neurother. 2016; 16:1427–41. DOI: 10.1080/14737175.2016.1209410 [PubMed: 27384886]

Huneau C, Benquet P, Dieuset G, Biraben A, Martin B, Wendling F. Shape features of epileptic spikes are a marker of epileptogenesis in mice. Epilepsia. 2013; 54:2219–27. DOI: 10.1111/epi.12406 [PubMed: 24134559]

Janca R, Jezdik P, Cmejla R, Tomasek M, Worrell GA, Stead M, et al. Detection of interictal epileptiform discharges using signal envelope distribution modelling: application to epileptic and non-epileptic intracranial recordings. Brain Topogr. 2015; 28:172–83. DOI: 10.1007/s10548-014-0379-1 [PubMed: 24970691]

Jerome Engel, J. Seizures and Epilepsy. Oxford Univ Press; 2013.

Karoly PJ, Freestone DR, Boston R, Grayden DB, Himes D, Leyde K, et al. Interictal spikes and epileptic seizures: their relationship and underlying rhythmicity. Brain. 2016; 139:1066–78. DOI: 10.1093/brain/aww019 [PubMed: 26912639]

Kerezoudis P, Grewal SS, Stead M, Lundstrom BN, Britton JW, Shin C, et al. Chronic subthreshold cortical stimulation for adult drug-resistant focal epilepsy: safety, feasibility, and technique 2017. J Neurosurg. 2017; :1–11. DOI: 10.3171/2017.5.JNS163134

Klimes P, Duque JJ, Brinkmann B, Van Gompel J, Stead M, St Louis EK, et al. The functional organization of human epileptic hippocampus. J Neurophysiol. 2016; 115:3140–5. DOI: 10.1152/jn.00089.2016 [PubMed: 27030735]

Krendl R, Lurger S, Baumgartner C. Absolute spike frequency predicts surgical outcome in TLE with unilateral hippocampal atrophy. Neurology. 2008; 71:413–8. DOI: 10.1212/01.wnl.0000310775.87331.90 [PubMed: 18614768]

Kucewicz MT, Cimbalnik J, Matsumoto JY, Brinkmann BH, Bower MR, Vasoli V, et al. High frequency oscillations are associated with cognitive processing in human recognition memory. Brain. 2014; 137:2231–44. DOI: 10.1093/brain/awu149 [PubMed: 24919972]

Li MCH, Cook MJ. Deep brain stimulation for drug-resistant epilepsy. Epilepsia. 2017; doi: 10.1111/epi.13964

Lundstrom BN, Van Gompel J, Britton J, Nickels K, Wetjen N, Worrell G, et al. Chronic Subthreshold Cortical Stimulation to Treat Focal Epilepsy. JAMA Neurol. 2016; 73:1370.doi: 10.1001/jamaneurol.2016.2857 [PubMed: 27654625]

Lundstrom BN, Worrell GA, Stead M, Van Gompel JJ. Chronic subthreshold cortical stimulation: a therapeutic and potentially restorative therapy for focal epilepsy. Expert Rev Neurother. 2017; 17:661–666. DOI: 10.1080/14737175.2017.1331129 [PubMed: 28532252]

Matsumoto A, Brinkmann BH, Matthew Stead S, Matsumoto J, Kucewicz MT, Marsh WR, et al. Pathological and physiological high-frequency oscillations in focal human epilepsy. J Neurophysiol. 2013; 110:1958–64. DOI: 10.1152/jn.00341.2013 [PubMed: 23926038]

Meisel C, Schulze-Bonhage A, Freestone D, Cook MJ, Achermann P, Plenz D. Intrinsic excitability measures track antiepileptic drug action and uncover increasing/decreasing excitability over the wake/sleep cycle. Proc Natl Acad Sci. 2015; 112:14694–9. DOI: 10.1073/pnas.1513716112 [PubMed: 26554021]

Miller JW, Kim W, Holmes MD, Vanhatalo S. Ictal localization by source analysis of infraslow activity in DC-coupled scalp EEG recordings. Neuroimage. 2007; 35:583–97. DOI: 10.1016/j.neuroimage.2006.12.018 [PubMed: 17275335]

Mormann F, Lehnertz K, Daivd P, Elger CE. Mean phase coherence as a measure for phase synchronization and its application to the EEG of epilepsy patients. Phys D. 2000; 144:358–69.

Neske GT. The Slow Oscillation in Cortical and Thalamic Networks: Mechanisms and Functions. Front Neural Circuits. 2015; 9:88.doi: 10.3389/fncir.2015.00088 [PubMed: 26834569]

Nir Y, Staba RJ, Andrillon T, Vyazovskiy VV, Cirelli C, Fried I, et al. Regional Slow Waves and Spindles in Human Sleep. Neuron. 2011; 70:153–69. DOI: 10.1016/j.neuron.2011.02.043 [PubMed: 21482364]

Nunez, PL., Srinivasan, R. Electric fields of the brain: the neurophysics of EEG. 2nd. Oxford; New York: Oxford University Press; 2006.

Press, WH. Numerical recipes in C: the art of scientific computing. 2nd. Cambridge; New York: Cambridge University Press; 1992.

Song I, Orosz I, Chervoneva I, Waldman ZJ, Fried I, Wu C, et al. Bimodal coupling of ripples and slower oscillations during sleep in patients with focal epilepsy. Epilepsia. 2017; 58:1972–84. DOI: 10.1111/epi.13912 [PubMed: 28948998]

Staley KJ, White A, Dudek FE. Interictal spikes: harbingers or causes of epilepsy? Neurosci Lett. 2011; 497:247–50. DOI: 10.1016/j.neulet.2011.03.070 [PubMed: 21458535]

Stead M, Bower M, Brinkmann BH, Lee K, Marsh WR, Meyer FB, et al. Microseizures and the spatiotemporal scales of human partial epilepsy. Brain. 2010; 133:2789–97. DOI: 10.1093/brain/awq190 [PubMed: 20685804]

Steriade M. Grouping of brain rhythms in corticothalamic systems. Neuroscience. 2006; 137:1087–106. DOI: 10.1016/j.neuroscience.2005.10.029 [PubMed: 16343791]

Thomas L, Bledsoe JM, Stead M, Sandroni P, Gorman D, Lee KH. Motor cortex and deep brain stimulation for the treatment of intractable neuropathic face pain. Curr Neurol Neurosci Rep. 2009; 9:120–6. [PubMed: 19268035]

Vanhatalo S, Palva JM, Holmes MD, Miller JW, Voipio J, Kaila K. Infraslow oscillations modulate excitability and interictal epileptic activity in the human cortex during sleep. Proc Natl Acad Sci U S A. 2004; 101:5053–7. DOI: 10.1073/pnas.0305375101 [PubMed: 15044698]

Velasco M, Velasco F, Velasco AL, Boleaga B, Jimenez F, Brito F, et al. Subacute electrical stimulation of the hippocampus blocks intractable temporal lobe seizures and paroxysmal EEG activities. Epilepsia. 2000; 41:158–69. [PubMed: 10691112]

Warren CP, Hu S, Stead M, Brinkmann BH, Bower MR, Worrell GA. Synchrony in normal and focal epileptic brain: the seizure onset zone is functionally disconnected. J Neurophysiol. 2010; 104:3530–9. DOI: 10.1152/jn.00368.2010 [PubMed: 20926610]

Wyllie, E., editor. Wyllie's Treatment of Epilepsy. 6th. Philadelphia, PA: Wolters Kluwer; 2015.
Zar, JH. Biostatistical analysis. 5th. Upper Saddle River, N.J.: Pearson Education; 2009.

Highlights

- Intracranial EEG is systematically compared between patient groups with and without seizures.
- Sharply contoured EEG activity may be more prevalent than expected in patients without seizures.
- EEG spiking and slow waves differ between patient groups with differing seizure probabilities.

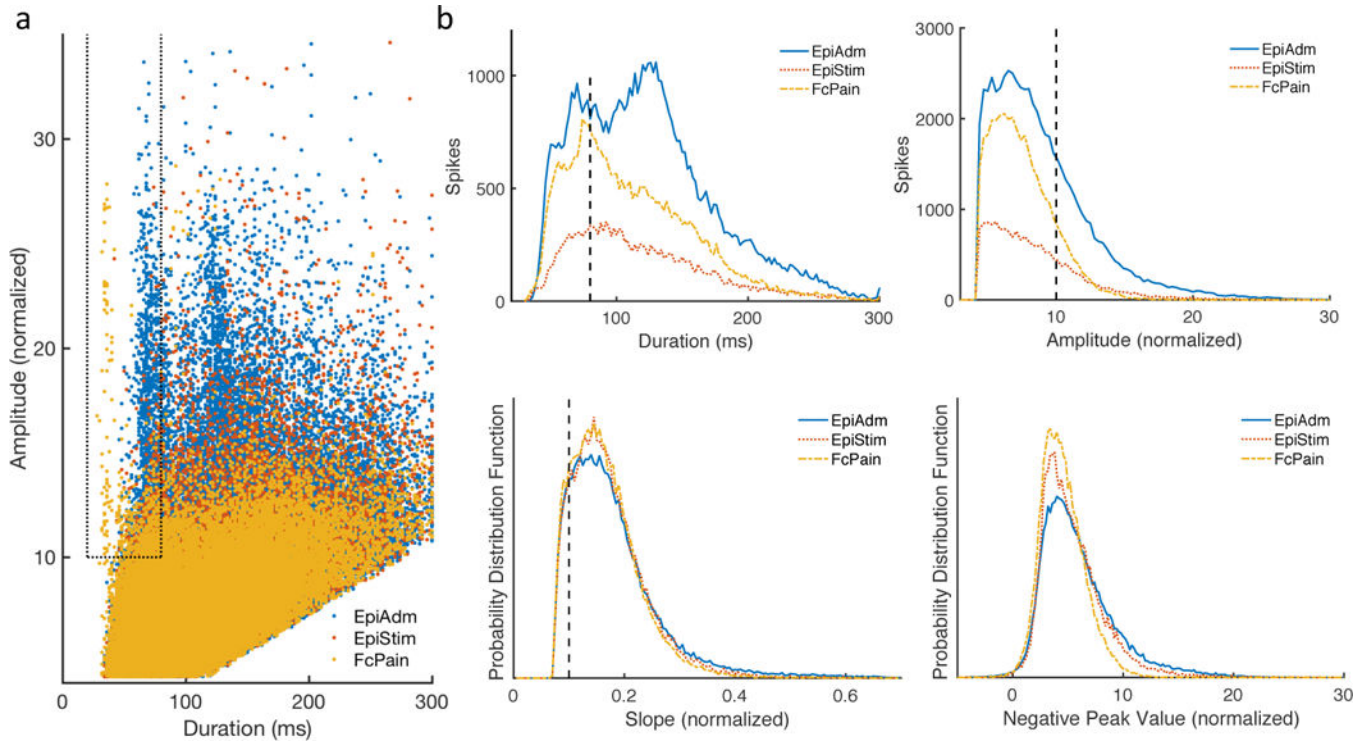

Figure 1.

Shape characteristics of sharply contoured waveforms and selection of spikes. **(a)** Scatterplot shows a small region encompassed by dotted lines of waveforms meeting the shape criteria for spikes. **(b)** Sharply contoured waveforms classified as spikes had a duration of 20–80 ms as well as an amplitude >10 and slope >0.1 with normalized units of grid median channel mean absolute amplitude.

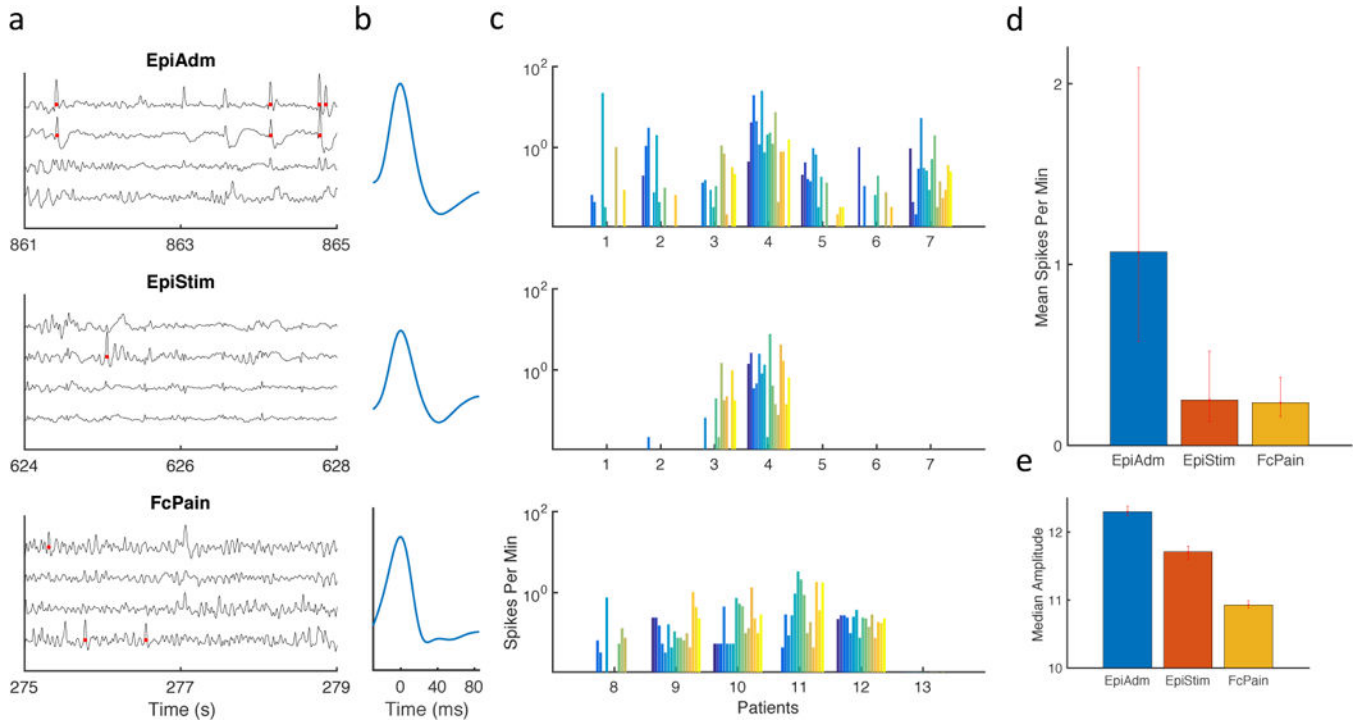

Figure 2.

Sharply contoured waveforms classified as spikes for three patient groups. **(a)** Example intracranial EEG traces are shown from subdural grids implanted in epilepsy patients at admission (EpiAdm), epilepsy patients undergoing continuous cortical stimulation (EpiStim), and patients with facial pain and no history of seizures (FcPain). Red dots indicate spikes detected via an automated method. **(b)** Average detected waveforms for the three groups are similar. **(c)** Spike rate for each of 16 electrodes were analyzed for each patient. **(d)** Mean spike rate for the grid was calculated for each patient. Mean spike rate from EpiAdm (n = 112; 1.07, [0.57 2.1]) was increased compared to EpiStim (n = 112; 0.25, [0.13 0.51]) and FcPain (n = 96; 0.24, [0.16 0.37]). **(e)** Spike amplitude differences were small but significant for EpiAdm (n = 10,803; 12.3, [12.24 12.38]), EpiStim (n= 2,521; 11.71, [11.60 11.79]), and FcPain (n= 2,243; 10.93, [10.89 10.99]). Units are normalized to the grid median time average of the absolute contact amplitude. Error bars represent 95% confidence intervals determined by bootstrapping.

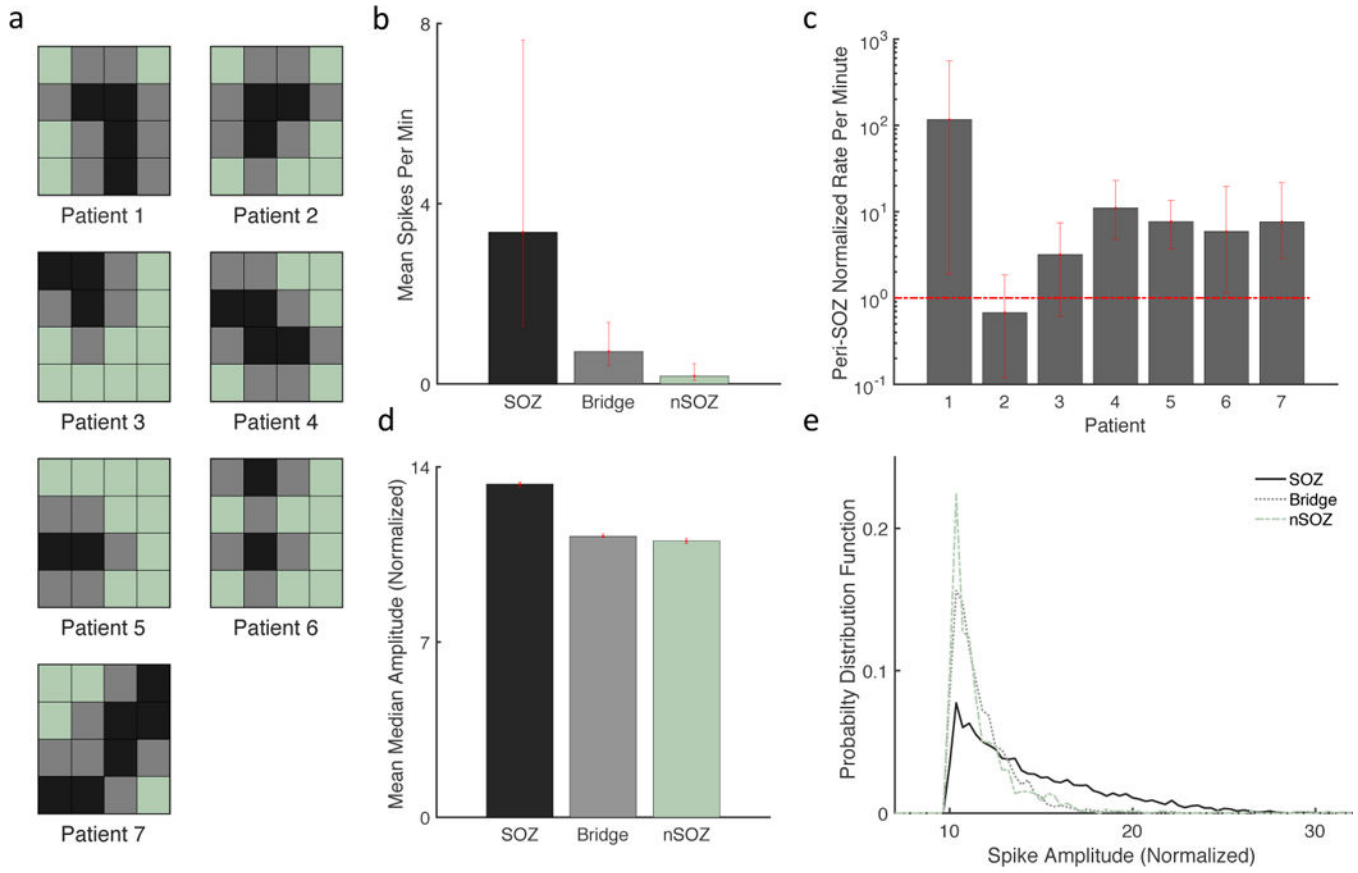

Figure 3.

Spike rates and amplitudes are increased in the SOZ compared to the nSOZ. **(a)** Diagrams of the 4×4 subdural grid for each patient. SOZ contacts are black, Bridge contacts are gray, and nSOZ contacts are light green. **(b)** Mean spike rate was increased for contacts in the SOZ (n = 24; 3.37, [1.27 7.56]) compared to the nSOZ (n = 45, 0.18, [0.08 0.46]), while Bridge contacts (n = 43, 0.72, [0.41 1.37]) had an intermediate spike frequency. **(c)** Mean spike rate of SOZ and Bridge contacts was normalized by the mean nSOZ rate for each patient. Rates greater than one (horizontal dashed red line) signify an increased rate in the peri-SOZ region. Rates were significantly increased for five of seven patients. **(d)** Spike amplitudes were increased for the SOZ (n= 7,280; 13.3 [13.20 13.41]) compared to Bridge (n = 2,791; 11.2, [11.18 11.32]) and nSOZ (n = 717; 11.0, [10.93 11.15]). **(e)** Very high amplitudes were present in the SOZ but not Bridge or nSOZ spikes, demonstrated by the long rightward tail of the SOZ probability distribution function. Error bars represent 95% confidence intervals determined by bootstrapping.

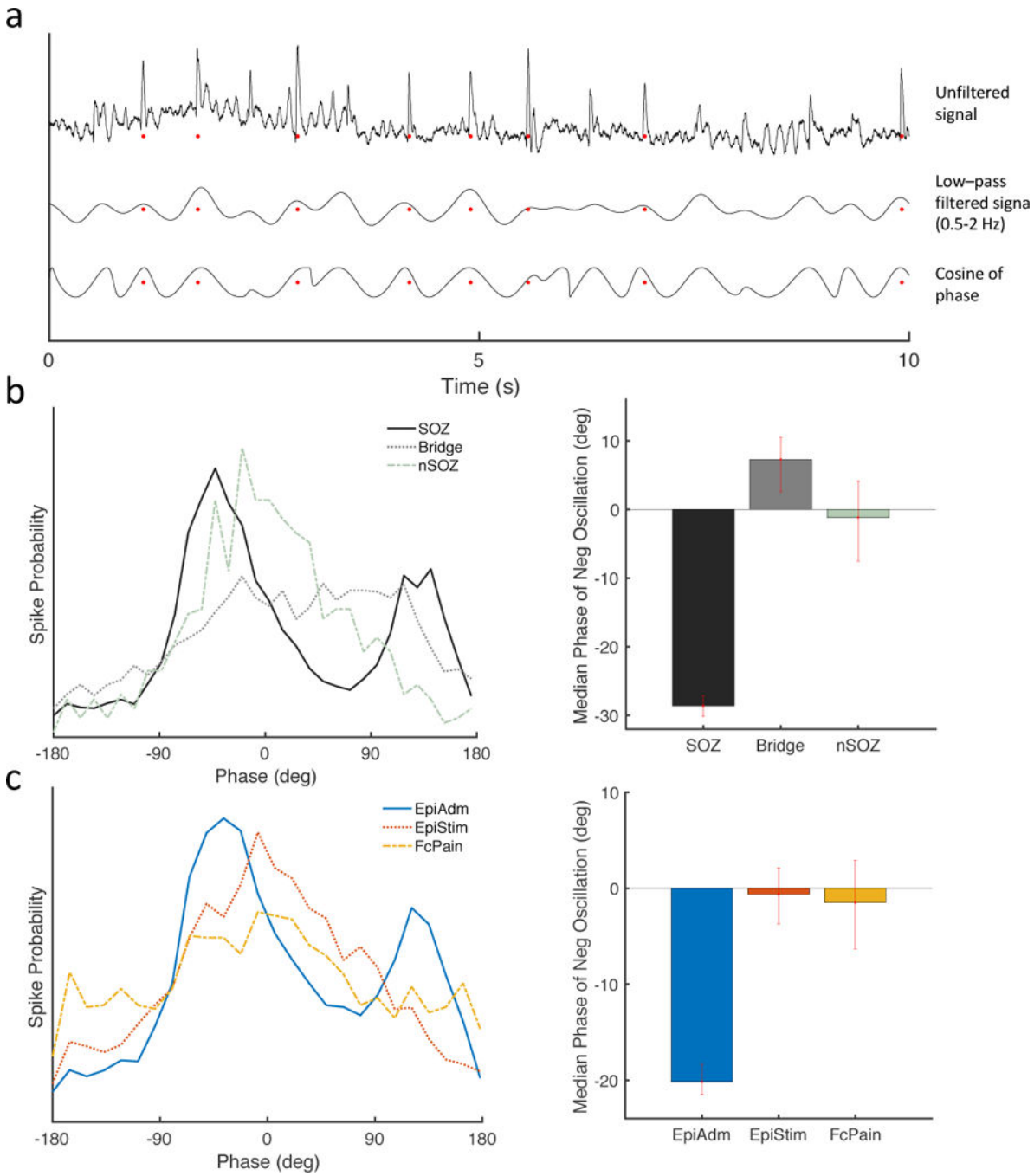

Figure 4.

Spikes occur earlier during the negative portion of slow oscillations. **(a)** Example traces of the unfiltered iEEG signal (top), the signal bandpass filtered at 0.5–2 Hz (middle), and the cosine of the phase (bottom). Red dots represent automatically detected spikes. Negative is upwards, and negative peaks correspond with phase of zero degrees. **(b)** Spikes in the SOZ occurred earlier (peak at −42 degrees) with respect to the phase of slow wave oscillations (0.5–2 Hz) than spikes in the nSOZ (peak at 20 degrees). Median phases during the negative slow oscillations occurred earlier for the SOZ (n=4,704; −28.6, [−30.1 −27.1]) compared to

Bridge (n=1,904, 7.3, [2.4 10.5]) and nSOZ (n=583; −1.2, [−7.5 4.1]). **(c)** Similarly, spikes in EpiAdm occurred earlier (peak −37 degrees) than spike from EpiStim (peak 8 degrees) or FcPain (peak 8 degrees). Median phases during the negative slow oscillations occurred earlier for the EpiAdm (n=7,191; −20.2, [−21.7 −18.5]) compared to EpiStim (n=1,872; −0.6, [−3.7 2.4]) and to FcPain (n=1,215; −1.5, [−6.5 2.2]). Error bars represent 95% confidence intervals determined by bootstrapping.

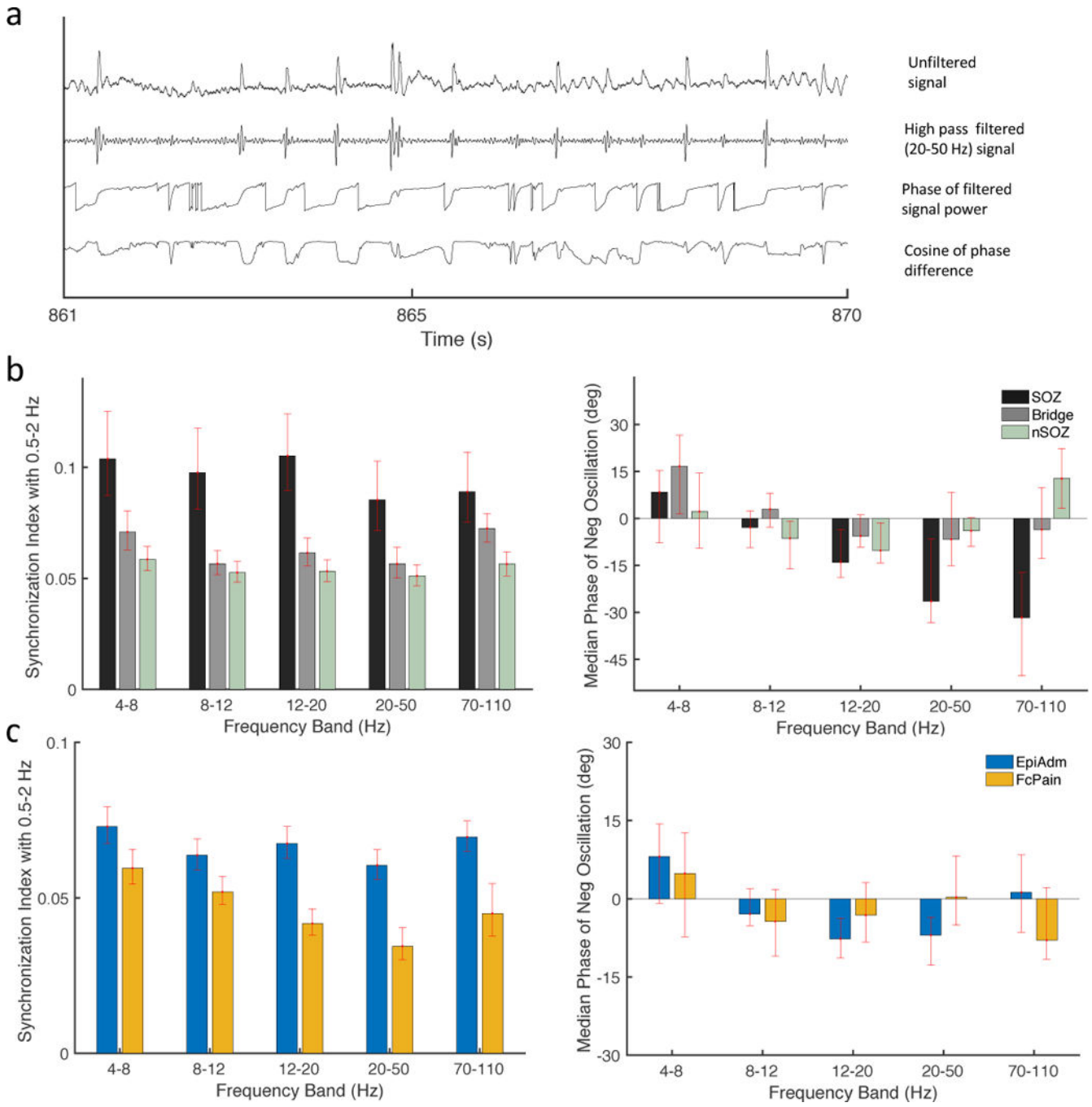

Figure 5.

Cross-frequency coupling between slow oscillations (0.5–2 Hz) and higher frequency oscillations. **(a)** Example traces of the unfiltered iEEG signal (top) and bandpass filtered iEEG data (lower traces). Red dots represent automatically detected spikes. Negative is upwards, and negative peaks correspond with phase of zero degrees. **(b)** Synchronization Index between slow oscillations and higher bandpass filtered signals shows significantly increased coupling between the SOZ compared to the nSOZ contacts for all frequencies. During the negative oscillation, the median slow oscillation phase for maximal coupling, or

preferred phase, was significantly earlier for 70–110 Hz (right panel). **(c)** Coupling was increased for EpiAdm compared to FcPain, with no significant differences for preferred phases during the negative oscillation (right panel). Error bars represent 95% confidence intervals determined by bootstrapping.

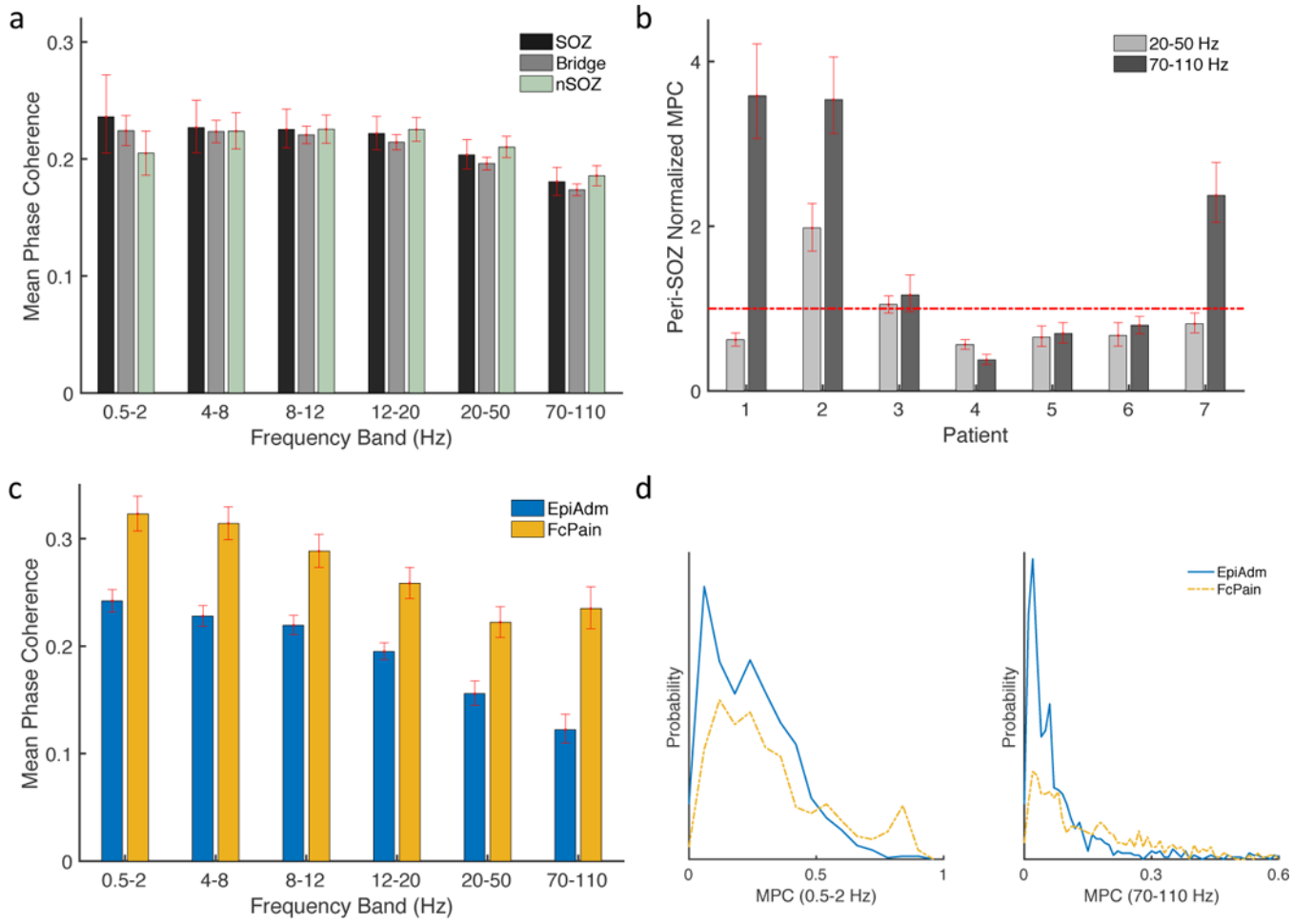

Figure 6.

Mean phase coherence (MPC) for adjacent electrode pairs. **(a)** MPC was not significantly diffferent for contacts in the nSOZ for frequencies 20–50 and 70–110 Hz. **(b)** MPC in SOZ and Bridge regions was normalized by MPC for nSOZ contacts. Values less than one signify increased synchrony in nSOZ contacts. **(c)** MPC was significantly decreased for EpiAdm compared to FcPain for all frequency bands. **(d)** Probability distributions of MPC values for adjacent contacts for the lowest and highest frequency bands are right-shifted for FcPain compared to EpiAdm. Error bars represent 95% confidence intervals determined by bootstrapping.

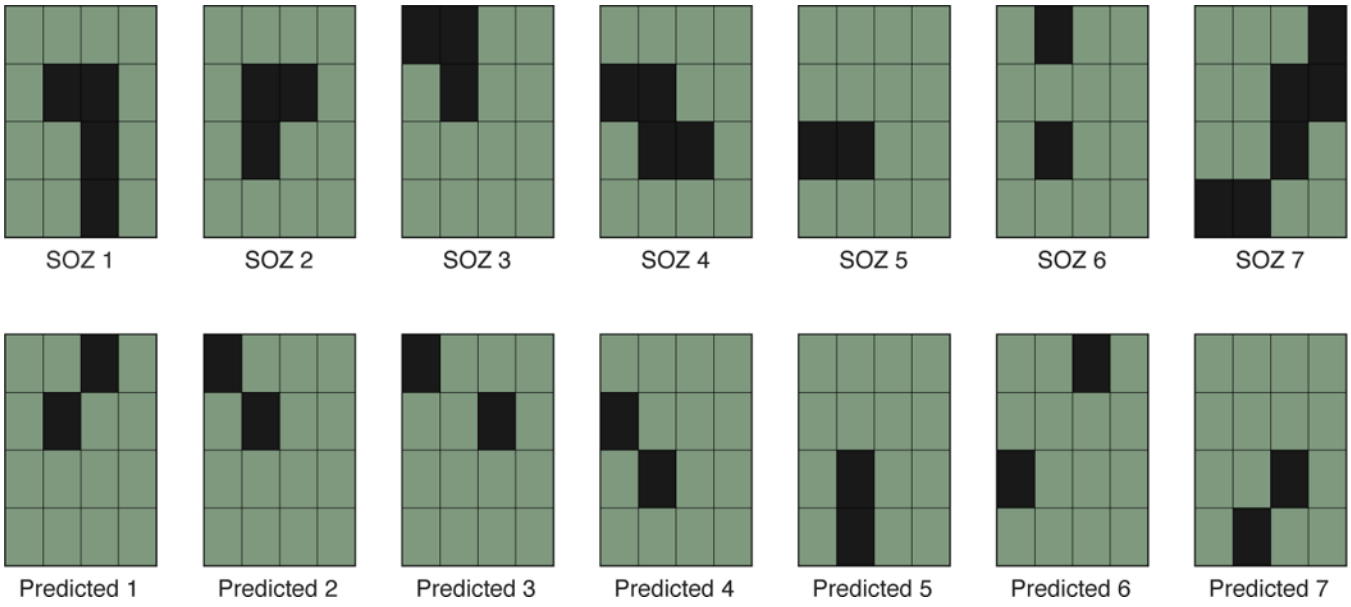

Figure 7.

Prediction of the two most likely contacts to be within the SOZ for each grid. Upper row shows the clinically determined SOZ (black squares) for each of the seven patients. Equally weighted measures (spike rate, spike amplitude, spike phase to slow oscillation, and synchronization index) were used to rank the electrodes of each grid. The top two electrodes for each grid are displayed in the lower row. Eight of 14 possible contacts were in the SOZ ($p = 0.003$ per Monto Carlo simulation $n = 10{,}000$).